
Uniformity of ac growth of copper nanowires within the porous alumina template from acidic Cu(II) sulphate solutions

Arūnas Jagminas*,
Aldona Jagminienė and
Eimutis Matulionis

*Institute of Chemistry,
A. Goštauto 9,
LT-2600 Vilnius, Lithuania
E-mail: jagmin@ktl.mii.lt

Experiments varying acidic Cu(II) sulphate solution composition and the template parameters at ac voltage control were performed to study the uniformity of growth of copper nanowires within the alumina pores. *Vis*-spectrometry analysis of copper content, electron probe microanalysis (EPMA) and scanning tunneling microscopy (STM) were employed. On the basis of the experimental results, it is suggested that non-uniform growth of copper nanowires is related to the hydrogen co-evolution process. H₂ bubbles plug the alumina pores as electrolysis progresses, preventing supply of the electroactive species and causing a sharp decrease in current density. To obtain a uniform filling of the alumina pores, a thinner barrier oxide layer, the optimal composition of Cu(II) solution and a linear increase of ac voltage at the onset of electrolysis are a prerequisite.

Key words: growth instability, self-assembled Cu⁰ nanowires, alumina, ac deposition

INTRODUCTION

Nanometer-sized metals and semiconductors are of great interest, because they exhibit valuable and unique physical and chemical properties which differ significantly from bulk materials [1–3]. Several methods have been proposed for the synthesis of nanostructures, such as electron- and ion-beam lithography [4], X-ray microlithography [5], scanning probe microscopy-based lithography [6], template [7–9], and sonochemical [10, 11] synthesis. Template synthesis entails deposition of a desirable material species composed of conductive polymers [12], semiconductors [13, 14], carbon nanotubes [15, 16], metals [17–19], their oxides [20, 21] and multilayered composites [22] into the pores of a nanoporous template.

Anodically grown porous oxide films, so-called alumina, have been known for decades as corrosion and heat resistant, light-fastness and hard coatings for Al surface finishing [23]. In the last decade they have been successfully used as filtration membranes [24], etching masks [25], and as a self-ordered template material [26–28]. The structure of porous alumina has been characterized in numerous works by a closed-packed array of columnar hexagonal cells, each containing an elongated central pore, normal to

the Al surface and separated from it by a barrier type layer with a thickness from 1.0 to 1.30 nm/V [29 and ref. cited herein]. The size of cells and pores in alumina linearly increases with increase in anodizing voltage [28, 30] and is affected by electrolyte concentration [31]. The pore concentration in alumina templates is in the order 10⁹ to 10¹¹ pores/cm² [23, 26–29, 31, 32]. Besides, high-ordered porous alumina templates with an almost ideal honeycomb structure can be grown on annealed, high purity and smooth Al surface [33] under certain anodizing conditions [9, 24–28, 31, 34].

Due to the rectifying properties of the alumina barrier layer, the alternating current has been used since the past to fill the alumina pores with different materials starting from the bottom without perforation of the alumina barrier layer. The transmission electron microscope and scanning tunneling microscope images of various metal particles (Fe, Ni, Co, Cd, Ag) liberated from the alumina layers indicated their columnar structure with approximately equivalent areas per volume. All this allowed Moskovits et al. [18] to conclude that metallic particles deposited by means of ac electrolysis faithfully reproduce the shape of the alumina pores.

Calculations and experiments have shown that the properties of nanostructured materials, such as

optical, electric, magnetic, catalytic, etc. strongly vary with their size and shape, even though they have the same composition [7, 22, 35]. Therefore, it is envisaged that in the future the ability to control the properties of nanoscale materials will be related with the ability to control the uniformity of the size of the particles and their distribution in the dielectric matrix. In the last decade, attention here has been focused more on the high-ordered porous alumina template growth [9, 26–28, 31, 33], expecting that the deposited species will faithfully reproduce the shape of the pores. The optimal ac deposition conditions of the material species in the alumina pores differ for various solutions and various templates, whereas under other conditions the phenomena such as alumina barrier oxide layer spalling [36], pitting corrosion [13], non-uniform material deposition leaving a considerable pore volume unoccupied [18], and the oxide film flaking or peeling off from the Al substrate [37] can take place. According to [38], the growing rate of the metal species under ac voltage control gradually decreases and finally the columns stop growing. Therefore, the pores are not fully filled with metals and the lengths of their columns are supposed to differ, although it is still unknown why the columns stop growing. Few investigations devoted to the uniform growth of metallic nanowires by means of pulse or ac deposition deal with the requirement to decrease the thickness of the alumina barrier oxide layer and increase the solution concentration [39–41].

In this paper we describe how the alumina template growth and ac treatment conditions influence the uniformity of copper nanowires growth in the alumina pores. Based on the obtained results, suitable physicochemical processes determining the non-uniform filling of the alumina pores were analyzed with a new insight.

EXPERIMENTAL

Materials, surface preparation and anodizing

Experiments were carried out using tag-shaped specimens ($30 \times 30 \times 0.075$ or $15 \times 15 \times 0.3$ mm) cut from a commercially pure aluminium (99.5% Al, 0.24% Fe, 0.2% Si, 0.03% Cu, 0.02% Zn and 0.01% Ti) foil or sheet. The surface of Al specimens before anodizing was etched in a hot 1.5 M NaOH solution for 15 s, neutralized in a 1.5 M HNO₃, carefully rinsed and air-dried. The cleaned specimens were anodized under dc voltage, U_a , control in a vigorously stirred aqueous 1.53 M sulphuric acid (18 ± 0.2 °C, U_a 15 V) or 0.4 M phosphoric acid (25 ± 0.2 °C, U_a 80 V) solutions. Different anodizing times up to 120 min were employed to

obtain a various template thickness, δ . Two Pb sheets or graphite plates were used in sulphuric and phosphoric anodizing baths, respectively, as cathodes. The thickness of the alumina barrier layer, δ_b , was reduced after the template formation by lowering the anodizing cell voltage in a series of small steps [45] (2.0–0.5 volt per 30 s) from U_a to final voltage, $U_{a,fin}$, equal to 40, 20, 13, 10 or 7 V. To increase δ_b of the alumina grown in the sulphuric acid bath, the following anodizing in the same bath but at 1 °C and 20 V for 30 s was conducted.

All solutions were prepared from triply distilled water, especially pure acids and chemical grade salts purchased from Aldrich. Only triethanolamine was purified additionally by distillation under reduced pressure at 200 °C.

Procedures

After formation and rinsing with flowing distilled water the alumina template was inserted into an aqueous acidic Cu(II) solution for deposition of copper. The solution containing 0.1–0.6 M CuSO₄, 0.02–0.3 M MgSO₄ or Al₂(SO₄)₃ and sulphuric acid to adjust the pH value to 1.7–1.1 was used. To achieve homogeneous filling of the alumina pores, the influence of tartaric and phosphoric acids was also studied. Ac electrolysis was carried out at a constant average voltage, U_v , measured with a voltmeter of the electromagnetic system. A 50 Hz peak-to-peak sine wave centered at 0.0 V ac was used. The average current, J , during copper deposition was measured with the ac ammeter of the electromagnetic system. Seven graphite rods placed symmetrically around the specimen in a 200 cm³ cell were used as an auxiliary electrode.

Analysis

To determine the amount of deposited copper, m_{Cu} , the specimens were thoroughly rinsed and soaked in triply distilled water for 180 s to remove Cu(II) solution ions from the alumina template. The amount of copper deposited into the alumina pores was determined after its complete dissolution from a 4.5 cm² total surface in HNO₃ : H₂O (1:2) solution (2 cm³) for 120–180 s. All solutions used for copper dissolution, sample rinsing and further double soaking in triply distilled water for 180 s were mixed together. Then, 3 cm³ of H₂SO₄ (1:1) and 2 cm³ of 1% sodium diethyldithiocarbamate were added to the solution which finally was diluted to 50 cm³ and analyzed quantitatively at a wave-length 450 nm using a Perkin Elmer Lambda 35 UV/VIS spectrometer. Reproducibility of the analysis was checked by 3 repeated experiments. Standard solutions were made from 99.999% grade copper. A linear

Beer–Lambert law calibration curve of absorbance vs mg/dm^3 copper was obtained using a series of standard copper concentrations between 2 and 60.

The distribution of aluminium and copper within the alumina cross-section was detected using SEM with an X-ray microanalysis probe. A JXA 50A scanning electron microscope equipped with an X-ray microanalysis unit with a monochromatic CuK_α X-ray source was used. Template sections attached to the aluminium substrate were prepared by usual procedures of mechanical polishing of the specimen slices with metallographic papers and alumina abrasive slurries of 1.0, 0.3 and 0.05 μm on a polishing microcloth.

High resolution STM (scanning tunneling microscopy) observation of the alumina surface morphology was carried out with a PicoSTM system (Molecular Imaging). The images were obtained by repeated scanning of the alumina surface placed in an argon-filled box (Miwa Industries), using the contact mode with a microcantilever made of silicon nitride (spring constant: 0.68 N m^{-1}) at room temperature.

The gas evolved during ac electrolysis was assembled as in the earlier work [65].

RESULTS AND DISCUSSION

Our experience in research of the deposition of copper nanoparticles into alumina template pores by means of ac electrolysis leads us to the observation that the amount of metal, m_{Cu^0} , deposited from the same solution depends not only on the ac voltage applied and electrolysis duration, t , but also on the template growth conditions. Firstly, the anodizing voltage, U_a , is important for the ac voltage value at which the reduction of electroactive species, further substrate anodizing and the oxide framework peeling off begin. Secondly, the results of the alumina pores ac filling are hinged on the film thickness, δ , since there always exists the δ below which the deposition of copper into alumina pores does not take place.

As is shown in Fig. 1, the quantity of copper deposited into alumina pores under ac voltage control increases close to linear with t only at the beginning of the process. Afterwards, the rate of copper deposition, equal to $\partial m_{\text{Cu}^0}/\partial t$, decreases continuously with t . The filling of the pores continues until copper deposition on top of the alumina surface begins or the alumina barrier oxide layer breakdown occurs. The onset of the former process, showed in Fig. 1 by the arrows, may be determined from an increase in copper deposition rate. For alumina templates grown in sulphuric bath with the thickness more than 9 μm , this is observed only at

ac voltages $U_v \geq 0.55 \times U_{a,\text{fin}}$. The further electrolysis results in uneven deposition of reddish-brown powder-like deposits onto the alumina surface and in the formation afterwards of a copper layer. In contrast, at lower ac voltages, ordinary at $U_v < 0.55 \times U_a$, the deposition of copper onto the surface of the alumina with thickness more than 9 μm is not observed up to 30 min electrolysis since, as seen from curve 1 in Fig. 1, the copper deposition gradually decreases approaching zero.

During Cu^0 nanowires growth in acidic Cu(II) solutions, the time dependencies of the electrical current were recorded and typical variations of the current-time, $J(t)$, under ac voltage control are shown in the inset of Fig. 1. Three types of $J(t)$ variations may be revealed depending on the composition of the acidic Cu(II) solution and ac voltage value. A decrease in the current density, j , from the onset of ac electrolysis to a constant value (curve 1) is common for acidic Cu(II) solutions if $U_v/U_{a,\text{fin}} < 0.55$. At higher ac voltages and in more acidic solutions a sharp fall of the current observed always at the onset of ac electrolysis is succeeded by a rise to an approximately constant value (curve 2) or through the peak (curve 3); the rise occurs the earlier, the higher ac voltage. Further, some oscillations of the current within $\pm 0.01 \text{ A dm}^{-2}$ can be observed when copper deposition on the top of the film surface begins. These oscillations become much higher when the barrier oxide layer breakdown or template peeling off comes into play.

The typical high-resolution STM image taken from the top of the alumina template at the initial

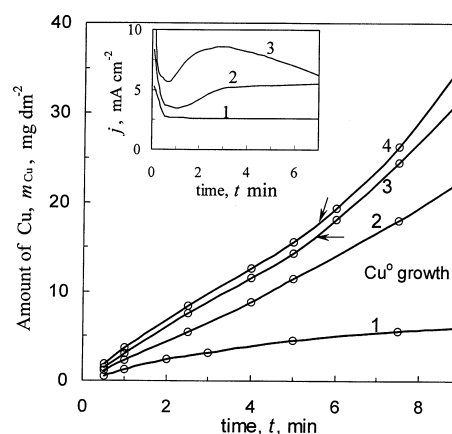


Fig. 1. Plots of amounts of Cu^0 deposited into alumina pores from solution containing 0.1 M CuSO_4 + 0.025 M $\text{Al}_2(\text{SO}_4)_3$ + H_2SO_4 up to pH 1.5 as a function of electrolysis time and ac voltage value: (1) 8; (2) 10; (3) 12; (4) 20 V. The alumina template with a thickness of $\sim 10 \mu\text{m}$ was grown in a sulphuric acid bath. The arrows indicate the onset of copper crystals growth at the alumina surface. In the inset – typical variations of ac current densities, j , observed during the growth of Cu^0 nanowires

moment of copper crystals growth onto the surface is shown in Fig. 2. The top view shows the mushroomed three-dimensional caps of copper nanowires emerging from mouths of some alumina pores implying that only part of the alumina pores are completely filled from acidic Cu(II) sulphate solution containing additionally MgSO_4 or $\text{Al}_2(\text{SO}_4)_3$ added to prevent the breakdown of the alumina barrier oxide layer [43]. These results are consistent with the copper distribution profiles obtained by EPMA of the Cu element in the cross-section of the alumina layer. As is shown in Fig. 3a, the amount of deposited copper was estimated to be highest at the bottom part of the pores and decreased with distance to the top, indicating fluctuations in the height of copper nanowires.

The filling of the alumina templates grown in a phosphoric acid bath at higher voltages is more problematic, since at higher ac voltages required in this case for copper deposition the alumina barrier oxide layer breakdown is inevitable. All attempts to fill such alumina pores by varying the solution pH,

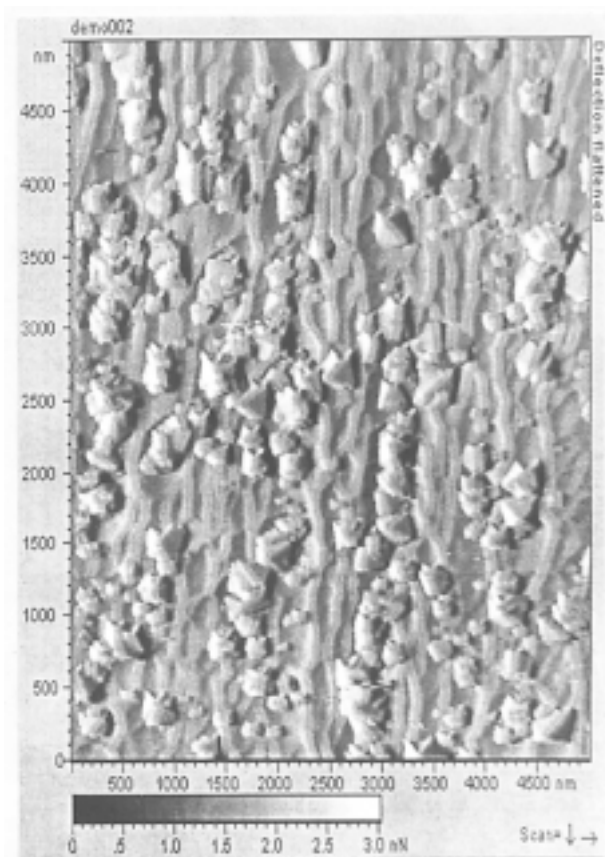


Fig. 2. Representative high resolution STM image of the alumina surface ($5 \times 5 \mu\text{m}$) showing caps of Cu^0 crystals grown only from part of the pores if a simple Cu(II) solution as in Fig. 1 and direct ac deposition are used. The alumina template was grown in a phosphoric acid bath for 2 h. $U_{a,\text{fin}} = 10 \text{ V}$, $U_v = 12 \text{ V}$

concentration, c , rather than U_v magnitude have failed. However, it has been established that the deposition of copper into the template pores proceeds easier from the same Cu(II) solution if the alumina barrier oxide layer thickness is decreased by lowering U_a . This is consistent with earlier observa-

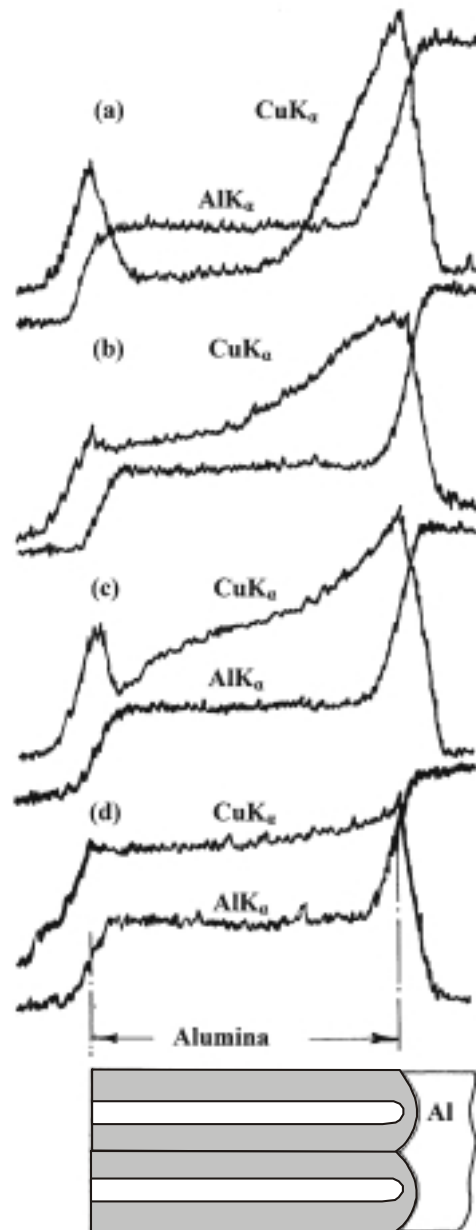


Fig. 3. (a) Distribution profiles of Al and Cu elements in the cross-section of alumina template grown in phosphoric acid bath at $U_a = 80 \text{ V}$ for 2 h after ac filling in the same solution as in Fig. 1 at $U_v = 32 \text{ V}$. The same EPMA results (b) show the alumina barrier layer thinning effect attained by lowering U_a to $U_{a,\text{fin}} = 10 \text{ V}$ since a much uniform growth of Cu^0 wires at $U_v/U_{a,\text{fin}} = 1.0$ is observed within the alumina with reduced δ_b . (c) and (d) –the same as (b) but after Cu^0 deposition in solution containing: $0.1 \text{ M CuSO}_4 + 0.05 \text{ M Al}_2(\text{SO}_4)_3 + 0.03 \text{ M tartaric acid} + \text{H}_3\text{PO}_4$ up to pH 1.5 without (c) and using a liner increase in $U_v/U_{a,\text{fin}}$ to 1.0 during the first 30 s (d)

tions while depositing Fe, Ni, Co [39], and Ag [40, 41] into the alumina templates by means of dc, ac and pulse electrolysis. The m_{Cu} against U_{v} plots for copper deposition from an acidic Cu(II) sulphate solution within the alumina template with approximately the same δ , but various δ_{b} are shown in Fig. 4. From these plots one can see that the behaviour of porous alumina with reduced δ_{b} manifests itself through parabolic dependencies of m_{Cu} against $U_{\text{v}}/U_{\text{a,fin}}$. The ratio of voltages at which copper deposition proceeds at a highest rate, $(U_{\text{v}}/U_{\text{a,fin}})_{\text{peak}}$, was found to increase with decreasing $U_{\text{a,fin}}$. However, at ac voltages higher than $(U_{\text{v}}/U_{\text{a,fin}})_{\text{peak}}$ (dashed lines in Fig. 4) the peeling off the alumina from the substrate and oxide spalling becomes critical. Therefore, attention here has been focused on the range of ac voltages which can be used for copper nanowires growth without the alumina barrier oxide layer breakdown; the range is the wider, the lower $U_{\text{a,fin}}$. This is valid also for the alumina templates grown in a sulphuric acid bath. Consequently, it seems difficult to estimate the optimal $U_{\text{v}}/U_{\text{a,fin}}$ for Cu^0 nanowires growth. Evidently, the optimal ac voltage is lower $(U_{\text{v}}/U_{\text{a,fin}})_{\text{peak}}$ and the final choice is up to a uniform filling of the alumina pores.

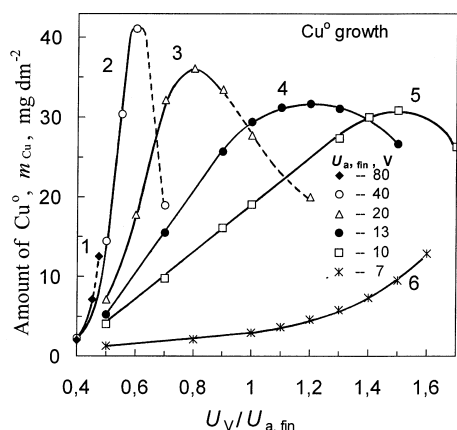


Fig. 4. Plots of amounts of Cu^0 deposited into alumina pores during 180 s by ac electrolysis as a function of the alumina barrier layer thinning conditions and $U_{\text{v}}/U_{\text{a,fin}}$ value. The solution containing 0.1 M CuSO_4 + 0.05 M MgSO_4 + H_2SO_4 up to pH 1.5 V was used. The alumina template was grown in phosphoric acid bath at $U_{\text{a}} = 80$ V for 1.5 h with a subsequent decrease in U_{a} to $U_{\text{a,fin}}$: (1) 80; (2) 40; (3) 20; (4) 13; (5) 10; (6) 7 V. The dashed lines correspond to the obvious damages of the alumina matrix

Electron probe microanalysis of copper distribution within the cross-section of the alumina template given in Fig. 3b shows the effect of the barrier oxide-layer-thinning. It is obvious that the uniformi-

ty of the pore filling increases with decreasing $U_{\text{a,fin}}$. For the alumina grown in sulphuric acid bath, the most uniform filling was obtained at $U_{\text{v}}/U_{\text{a,fin}} \approx 1.0$.

Seeking to increase the uniformity of copper nanowires growth, the influence of various additives on the m_{Cu} and Cu^0 distribution profiles across the alumina template were studied. The results concerning the influence of these additives on the copper deposition process from the acidic Cu(II) sulphate solution are depicted in Fig. 5. These results pointed out to the fact that varying the solution composition it is possible to increase the concentration of the solution up to 0.4 M without waste in the copper deposition rate. In addition, these experiments confirmed also a more uniform filling of the alumina pores up to the template surface (Fig. 3c). It must also be noted that acidic Cu(II) sulphate solutions containing TEA or urea and H_3PO_4 allowed us to deposit copper in thinner templates, commencing from 0.3–0.5 μm , than the solutions without additives where at least 2.5 to 3.0 μm template thickness is required [44].

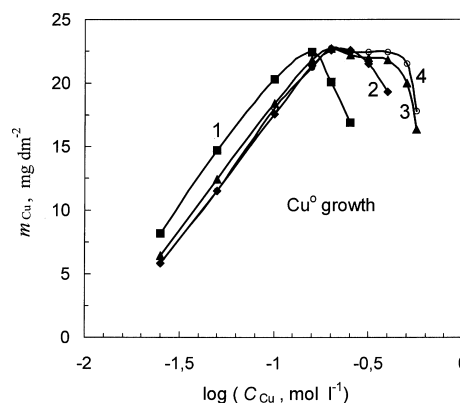


Fig. 5. Variations of m_{Cu} deposited during 300 s into alumina pores at ac $U_{\text{v}} = 10$ V on the concentration of CuSO_4 solution, $c_{\text{Cu}^{2+}}$ containing 0.025 M $\text{Al}_2(\text{SO}_4)_3$ and: (1) H_2SO_4 ; (2) H_3PO_4 ; (3) 0.03 M tartaric acid + H_2SO_4 ; (4) 0.03 M tartaric acid + H_3PO_4 . pH = 1.5. The matrix was grown in a sulphuric acid bath. $\delta = 9 \mu\text{m}$

At present, there is no clear experimental evidence for the reasons of either retarded or interrupted growth of the metal columns in some fractions of the pores. In the recent work, Sauer et al. [41] suggested that the uneven growth of silver wires within the alumina matrix by current pulse deposition technique is related to differences in the potential drops across the barrier oxide layer beneath the fraction of the pores due to electrostatic instabilities existing in this layer. However, it should be noted that although the resistance of the alumina barrier oxide in sites beneath the pores can be more

or less uneven due to some inhomogeneities, as can be seen from Fig. 3a, it is practically not influenced in copper deposition at the beginning of the process into the most, if not all, pores. It is also unreasonable to assume that the interrupted growth of the metal columns might be related to alumina pore sealing [45], especially for the alumina templates grown in a phosphoric acid bath since phosphate ions incorporated into the oxide film structure prevent pore sealing [23]. On the other hand, an interrupted and retarded growth of copper nanowires cannot be associated with an uneven decrease in the thickness of the barrier oxide layer as ac electrolysis progressed due to its damage by the side overall reaction $2\text{AlOOH} + 2e^- \rightarrow 2\text{AlO}_2^- + \text{H}_2$ or “shortering out” in a fraction of the pores [46]. As is seen from the inset of Fig. 1, the current during Cu^0 nanowires growth usually decreases at the onset of the process.

Variations of j against t can be regarded as a proof that ac-conductivity of the alumina template decreases when copper deposition progresses. These observations could be understood if we consider the up to tenfold increase in the electrode resistance in a manner corresponding to $j(t)$ plots. As has been shown recently [41], the resistance of the alumina barrier oxide layer prior to copper deposition, R_b , is three to four orders of magnitude higher than other resistances taken together in the copper deposition cell. On the other hand, it is well-known that R_b is directly related to $U_{a,\text{fin}}$ [23]. Therefore, it is reasonable to suggest that R_b ought to change its parameters proportionally to the ac peak voltage, U_p , already during the first 20–30 s causing changes in the barrier oxide layer ac-conductivity. The recent studies of the alumina template resistance and capacitance variations in the metal salt solutions with ac electrolysis conditions confirmed this assumption [47]. Therefore, the sharp decrease in the current at the onset of Cu^0 growth within a wide range of ac voltages, especially at ac peak voltage lower than $U_{a,\text{fin}}$, cannot be explained in terms of increase in the resistance of the alumina barrier oxide layer. Clearly another approach is required.

The observations on Cu^0 growth within the alumina pores are expected to be interpreted here based on the well-known fact that both reduction reactions of Cu^{2+} and H_3O^+ ions take place in acidic Cu(II) solutions during ac electrolysis [48].

A decrease in the current with an increase in time observed after a sharp rise (inset in Fig. 1) reflects the decrease in the rate of electrochemical reactions occurring at the oxide|solution at the bottom of the alumina pores and at the metal|oxide interfaces. Due to a valve character of alumina films to pass readily electrons from the metal to the so-

lution [23], this is most probably attributed to the reactions occurring in the cathodic ac period, especially for $U_v \leq 0.75 \times U_{a,\text{fin}}$ [49]. Voltammograms recorded in acidic Cu(II) solutions using the alumina template grown in a sulphuric acid anodizing bath have been analyzed recently in a separate paper [48] concluding that the main side reaction under potential sweep in cathodic direction is the protons reduction occurring before copper ion discharge. Therefore, it is reasonable to assume that hydrogen gas bubbles plug part of the alumina pores causing a drop in the total current due to a sharp decrease in the actual surface of electrochemical reactions. To verify these considerations, the current transients during 90 s ac electrolysis under voltage control and switch off for 180 s were recorded. As is seen in Fig. 6, a much higher current flows at the onset of each impulse and falls off later in a similar manner. The increase in the current after a delay in electrolysis time can be explained by an increase in the electroactive surface area due to degassing of the alumina template.

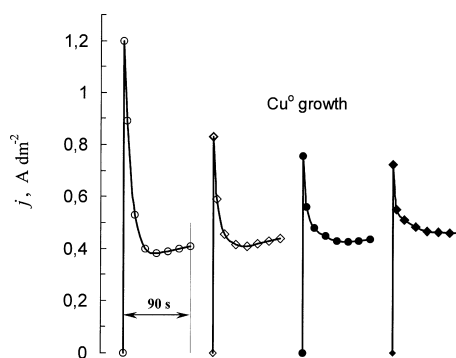


Fig. 6. Typical ac current profiles for the first 4 cycles of copper deposition into alumina pores at constant U_v 12 V from the same solution as in Fig. 4

For this reason the gas volumes evolved during Cu^0 nanowires growth were determined. The results obtained are shown in Table. It is evident that the volume of hydrogen gas, V_{H} , evolved from the same Cu(II) sulphate solution at the same $U/U_{a,\text{fin}}$ is related with the δ_b ; the lower $U_{a,\text{fin}}$, i.e. the thinner δ_b , the lower V_{H} . This effect explains the requirement to decrease δ_b of the alumina films in order to deposit various metals at the pores more uniformly [41, 45]. Although the reasons for this phenomenon are not yet clear, we suppose that this is probably due to changes in the transfer mechanism of the electrons through thick and thin oxide layers [50].

On the basis of these results it can be concluded that to obtain a homogeneous filling of alumina nanoscale pores by copper wires the hydrogen evolution should be avoided or maximally retarded

Table. Experimental values of the gas volume evolved during 3 min ac treatment of alumina in solution containing 0.1 M CuSO₄ + 0.02 M MgSO₄ + H₂SO₄ up to pH = 1.50 on the ac voltage U_v and the template growth final voltage U_{a,fin} in 0.4 M H₃PO₄ solution (U_a = 80 V, 25 °C, 1.5 h)

dc U _{a,fin} , V	7	10	13	20	40
ac U _v , V	6.3	9.0	11.7	18.0	36.0
U _v / U _{a,fin} ratio	0.9	0.9	0.9	0.9	0.9
V _{gas} , cm ³ /dm ²	0.2	0.85	1.75	3.1	11.2

from the beginning of the deposition process, using a suitable ac electrolysis regime and composition of Cu(II) solution. Therefore, ac voltage control, especially at the beginning of the process, and lower current densities should be used to evade intense hydrogen co-evolution. Based on this consideration it has been found that the optimal ac current densities, j_{opt} , for a uniform growth of copper nanowires varies between 0.3 to 0.45 A dm⁻² depending on the composition of Cu(II) solution; j_{opt} decreases with a decrease in the solution pH and increase in U_{a,fin}.

Last but not least, it has been determined that a high uniformity of filling the alumina pores with copper can be obtained using a linear increase in the voltage at the onset of the process during the first 30 to 40 s, the complex acidic Cu(II) solution and the template δ_b thinning procedure (Fig. 3d).

CONCLUSIONS

This work demonstrates that a decrease in the rate of copper nanowires growth within alumina pores from acidic Cu(II) sulphate solution as ac electrolysis progressed and non-uniform growth of metallic columns are related with hydrogen co-evolution process. The gas bubbles plug the alumina pores preventing supply of electroactive species to the discharge places and causing a sharp decrease in the current density. To obtain a uniform filling of the alumina pores, a thinner barrier oxide layer, more complex Cu(II) sulphate solution composition and a linear increase in the ac voltage up to the optimal U_v / U_{a,fin} ratio at the onset of the electrolysis are a prerequisite.

Received 24 October 2003
Accepted 10 November 2003

References

1. A. M. Morales and C. M. Lieber, *Science*, **279**, 208 (1998).

2. S. Frank, P. Poncharal, Z. L. Wang and W. A. de Heer, *Science*, **280**, 1744 (1998).

3. J. Xu, M. Ouyang, P. Yang and C. M. Lieber, *Nature*, **399**, 48 (1999).

4. F. K. Perkins, E. A. Dobisz and S. L. Brandow, *Appl. Phys. Lett.*, **68**, 550 (1996).

5. W. Chu, C. C. Eugster, A. Moel, E. E. Moon, J. A. Delalampo, M. Z. Schattenburg, K. W. Rhee, M. C. Peckerrar and M. R. Melloch, *J. Vac. Sci. Technol.*, **B 10**, 2966 (1992).

6. D. H. Huang, T. Nakayama and M. Aono, *Appl. Phys. Lett.*, **73**, 3360 (1998).

7. D. AlMawlawi, N. Coombs and M. Moskovits, *J. Appl. Phys.*, **70**, 4421 (1991).

8. C. R. Martin, *Science*, **266**, 1961 (1994).

9. H. Masuda and M. Satoh, *Jpn. J. Appl. Phys.*, **35**, L126 (1996).

10. S.-H. Yu, M. Yoshimura, J. M. C. Moreno, T. Fujiwara, T. Fujino and R. Teranishi, *Langmuir*, **17**, 1700 (2001).

11. R. V. Kumar, E. Elgamiel, Y. Diamant and A. Gedanken, *Langmuir*, **17**, 1406 (2001).

12. R. Parthasarathy and C. R. Martin, *Nature*, **369**, 298 (1994).

13. D. Routkevich, T. Bigioni, M. Moskovits and J. M. Xu, *J. Phys. Chem.*, **100**, 14037 (1996).

14. R. J. Tonucci, B. L. Justus, A. J. Campillo and C. E. Ford, *Science*, **258**, 783 (1992).

15. J. Li, M. Moskovits and T. L. Haslett T., *Chem. Mater.*, **10**, 1963 (1999).

16. Z.-h. Yuan, H. Huang, L. Liu and S.-s. Fan, *Chem Phys. Lett.*, **345**, 39 (2001).

17. W. Sautter, G. Ibe and J. Meier, *Aluminum*, **50**, 143 (1974).

18. C. K. Preston and M. Moskovits, *J. Phys. Chem.*, **97**, 8495 (1993).

19. D. G. W. Goad and M. Moskovits, *J. Appl. Phys.*, **49**, 2929 (1978).

20. Y. Ishikawa and Y. Matsumoto, *Electrochim. Acta*, **46**, 2819 (2001).

21. A. Jagminas, J. Kuzmarskytė and G. Niaura, *Appl. Surf. Sci.*, **201**, 129 (2002).

22. P. R. Evans, G. Yi and W. Schwarzacher, *Appl. Phys. Lett.*, **76**, 481 (2000).

23. J. Diggle, F. Downie and C. Goulding, *Chem. Rev.*, **69**, 365 (1969).

24. H. Masuda, K. Yasyi and K. Nishio, *Adv. Mater.*, **12**, 1031 (2000).

25. D. Crouse, Y.-H. Lo, A.E. Miller and M. Crouse, *Appl. Phys. Lett.*, **76**, 49 (2000).

26. H. Masuda and K. Fukuda, *Science*, **268**, 1466 (1995).

27. H. Masuda, F. Hasegawa and S. Ono, *J. Electrochem. Soc.*, **144**, L127 (1997).

28. A. P. Li, F. Müller, A. Birner, K. Nielsch and U. Gösele, *J. Appl. Phys.*, **84**, 6023 (1998).

29. R. C. Furneaux, G. E. Thompson and G. C. Wood, *Corros. Sci.*, **18**, 853 (1978).

30. R. C. Furneaux, W. R. Rigby and A. P. Davidson, *Nature*, **337**, 147 (1989).

31. A. Jagminas, D. Bigelienė, I. Mikulskas and R. Tamošiūnas, *J. Cryst. Growth*, **233**, 591 (2001).

32. T. Takahashi and M. Nagayama, *J. Chem. Soc. Jpn.*, **36**, 34 (1968).

33. R. E. Ricker, A. E. Miller, D.-F. Yue, G. Banerjee and S. Bandyopadhyay, *J. Electron. Mater.*, **25**, 1585 (1996).
34. O. Jesensky, F. Müller and U. Gösele, *Appl. Phys. Lett.*, **72**, 1173 (1998).
35. G. J. Strijkers, J. H. J. Dalderop, M. A. A. Broeksteeg, H. J. M. Swagten and W. J. M. de Jonge, *J. Phys. Chem.*, **95**, 5141 (1999).
36. P. G. Sheasby and W. E. Cooke, *Trans. IMF*, **52**, 103 (1974).
37. A. S. Doughty, G. E. Thompson, J. A. Richardson and G. C. Woods, *Trans. IMF*, **53**, 33 (1975).
38. M. Saito, M. Kirihara, T. Toniguchi and M. Miyagi, *Appl. Phys. Lett.*, **55**, 607 (1989).
39. P. M. Poulus, F. Luis, M. Kröll, G. Schmid and L. J. de Jongh, *J. Magn. Magn. Mater.*, **224**, 180 (2001).
40. T. Xu, G. Zangari and R. M. Metzger, *Nano Lett.*, **2**, 37 (2002).
41. G. Sauer, G. Brehm, S. Schneider, K. Nielsch, R. B. Wehrspohn, J. Choi, H. Hofmeister and U. Gösele, *J. Appl. Phys.*, **91**, 3243 (2002).
42. A. Jagminas, J. Giedraitienė and A. Selskis, *Chemija* (Vilnius), **11**, 3 (2000).
43. A. Jagminas, *J. Appl. Electrochem.*, **32**, 1201 (2002).
44. A. Jagminas and J. Reklaitis, *Zashch. Met.*, **22**, 821 (1986).
45. A. J. Yin, J. Li, W. Jian, A. J. Bennet and J. M. Xu, *Appl. Phys. Lett.*, **79**, 1039 (2001).
46. A. Zagieli, P. Natishan and E. Gileadi, *Electrochim. Acta*, **35**, 1019 (1990).
47. A. Jagminas, *Chemija* (Vilnius), **14**, (2003) (in press).
48. V. Skominas, S. Lichusina, P. Miecinskas and A. Jagminas, *Trans. IMF*, **79**, 213 (2001).
49. A. Jagminas and J. Reklaitis, *Trans. IMF*, **81**, 98 (2003).
50. J. C. Fischer and J. Giaever, *J. Appl. Phys.*, **32**, 172 (1961).

A. Jagminas, A. Jagminienė, E. Matulionis

**VARIO NANOSIŪLELIŲ ELEKTROCHEMINIO
AUGIMO AKYTOJE ALUMINA MATRICOJE
TOLYGUMAS**

S a n t r a u k a

Spektrometrinės analizės, elektronų zondo mikroanalizės bei STM metodais tirtas vario nanosiūlelių augimo aluminio anodinio oksido (alumina) matricių akutėse tolygumas. Nustatyta, kad rūgščiuose Cu(II) tirpaluose kintamosios srovės pastovaus įtampos kritimo (U_p) sąlygomis alumina matricos akutės užsipildo nevienodo ilgio metalinio vario siūleliais. Elektrolizės pradžioje varis sėda visose (ar daugumoje) akučių, tačiau vėliau šis augimas kai kuriose jų sulėtėja arba sustoja. Tai siejama su proceso metu kartu besiskiriančių dujų įtaka: dujos kaupiasi oksidinės matricos kapiliaruose ir ilgainiui dalį jų užkemša. Parodyta, kad, parenkant Cu(II) tirpalo priedus, nuosekliai didinant proceso pradžioje U_p bei suploninus alumina barjerinio sluoksnio storį, matricos akutes galima užpildyti nanometrinio skersmens vario siūleliais kur kas tolygiau.